Modelling and Simulation of Multiphase IM with Sinusoidal Flux Distribution used in Naval Applications including Torque Calculation

Carsten Heising, Jie Fang, Roman Bartelt, Volker Staudt and Andreas Steimel
Ruhr-University Bochum
D-44780 Bochum
Germany
Tel.: +49 234 32 23890
Fax.: +49 234 32 14597
Email: heising@eele.rub.de, fang@eele.rub.de, bartelt@eele.rub.de, staudt@eele.rub.de, steimel@eele.rub.de

***Abstract*—To guarantee high availability of naval drives and power-supply systems, error scenarios have to be simulated. The chosen differential-equations set has to represent the physical behaviour of complex naval induction machines, e.g. with 5- or 7- phase or double-star stator windings including asymmetric faults which is not featured by any simplified single-phase ECD.**

After a brief introduction of used simulation concept and modelling approach for motor drives with sinusoidal flux distribution, the torque calculation for n stator and m rotor windings is presented. The performance is demonstrated with the simulation of a five-phase induction machine emulating a single-phase failure.

I. Introduction

Stable operation of onboard grids and harbour-ship power supplies with high availability is a major concern in naval applications. To avoid stability problems and to prove the conceived redundancy of the chosen topology before erection and commissioning, the complex power-electronic systems in use today have to be simulated with high accuracy. To perform a simulation providing sufficient results, several requirements have to be fulfilled: On the one hand a simulation concept featuring multiterminal power-electronic systems is needed [1]. In detail such systems consist of power-electronic switching devices, continuous elements, different sampling and switching times and several independent dedicated control-hardware instances [2]–[4]. On the other hand all continuous elements have to be modelled in detail - e.g. busbars, power cables, generators and motor drives.

In this paper the focus is laid on the torque calculation for complex motor drives. In contrast to standard drive applications – in which a simplified one-phase ECD fulfils the accuracy requirements – in ship technologies more complex induction machines are used, e.g. induction machines with 5- or 7- phase or double-star stator windings. Furthermore, to raise availability, machines with more than three phases can be reconfigured to be operated with faults in one of the phases. To simulate such error scenarios the chosen set of differential equations has to model the physical behaviour of asymmetric machines which is not featured by any simplified single-phase ECD. Based on the chosen simulation concept, the total system reaction – including the transient behaviour of the machine torque – upon an occurring failure in a power-electronic switching device can be analysed in detail.

A simulation concept fulfilling the mentioned requirements is introduced briefly. Afterwards, a method of modelling complex induction machines featuring asymmetric characteristics of all stator and rotor parameters is described. Based on the chosen modelling approach, the torque is derivated in an arbitrary way. Simulation results of a five-phase induction machine emulating an occurring inverter error in one phase are shown, outlining the excellent usability of the presented modelling approach.

II. Structure of the simulation

Even to model the simple system of a machine inverter attached to an induction machine (IM) with m stator windings, the simulation has to deal with continuous elements (for example voltage sources, inductivities and capacitors) as well as with discrete parts, like switching power semiconductors. The state-space notation is used to model the continuous part. The set of i first-order differential equations is solved by the Bulirsch-Stoer implementation of the Richardson Extrapolation [5], [6], supported by an adaptive step-size algorithm. For the discrete part (e.g. the converter phase legs) Petri Nets are used. Each phase leg is described by its own Petri Net leading to a total of $5 \cdot m$ different states. With a classical 'state machine' 5^m different states would be necessary to describe the IM with attached inverter. Furthermore, the Petri Net modulation based on the net-array description is easier to compute with modern personal computers.

This simulation framework – programmed in 'C++' language – allows very fast and accurate simulation of the overall system. A special advantage of the simulator allows the control algorithm to be used identically in simulation and in real-time control. This is possible because the simulator enables the use of C-code and emulates the whole control-hardware structure, thus minimizing development time-losses

978-1-4244-8218-4/10/$26.00 ©2010 IEEE

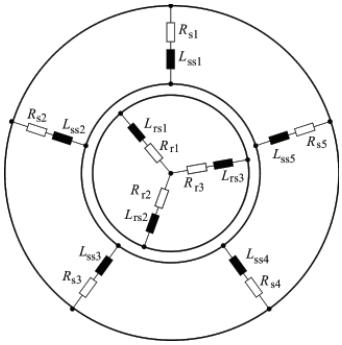

Fig. 1. Example with $m = 5$ stator and $n = 3$ rotor windings

by program portation.

III. System under analysis

The main aspect of the chosen approach is to model IM by concentrated elements known of the standard IM-ECD and leakage inductance voltage drops. In contrast to common modelling approaches, the influence of each single component in stator and rotor is taken into account. In consequence, asymmetric IM can be modelled.

Because of the different time scales, the frequency of rotation ω and the angular rotor position χ are not included in the derived state-space equations, leading to linear and time-invariant characteristics. Instead they are taken into account by additional differential equations.

To achieve a model which is very close to physical reality the flux distribution of the IM has to be computed based on functions of the current linkage of each single winding [7]. In high-power induction-machine applications this distribution can be assumed to have sinusoidal shape. Another assumption, also leading to a negligible error, is to set the permeability of the iron core to infinity and to ignore the parasitic interaction between the different winding systems.

Using these assumptions induction machines can be modelled using the leakage induction voltage drops in rotor and stator. These voltage drops result from the differences between the terminal voltages and the sum of the induced voltages and the winding resistance (cp. Fig. 1).

$$L_\sigma \frac{di_\sigma}{dt} = u_t - (R_\sigma \cdot i_\sigma + u_{ind}) \tag{1}$$

The terminal voltages u_t are input signals. The induced voltages u_{ind} have to be calculated for each single winding. Thus, the change of the flux linkage in each winding has to be identified which can be realised using the superposition principle.

In detail the flux created by the particular examined winding system l is superposed by the fluxex of each winding (stator and rotor) effective at this position. The relevant quantities are the actual magnitude of the flux $\hat{\psi}_{l,k}(t)$ created by the winding system k and the angle $\theta_{l,k}(t)$ between the winding systems l and k (with $l, k \in [s_1, \ldots, s_m, r_1, \ldots r_n]$).

$$\psi_{l,k}(\theta_{l,k}, t) = \hat{\psi}_{l,k}(t) \cdot \cos(\theta_{l,k}(t)) \tag{2}$$
$$= L_k \cdot i_k(t) \cdot \cos(\theta_{l,k}(t)) \tag{3}$$

Here L_k includes the number of turns. The angle $\theta_{l,k}(t)$ consists of a constant angle $\theta_{geom,k}$ due to the geometry of the IM and a time variant angle $\chi(t) = \int \omega dt$ which is caused by the rotation ω of the IM rotor. The overall flux effective in winding system l can be calculated to

$$\psi_{\Sigma,l}(t) = \sum_{k=s_1}^{s_m} \psi_{l,k}(t) + \sum_{k=r_1}^{r_n} \psi_{l,k}(t) \tag{4}$$

To reduce the complexity of the derived equations the arithmetic constraint of Kirchhoff's current law $\sum i = 0$ will be used at the end of the derivation.

Using the model of an IM with $m = 5$ stator and $n = 3$ rotor windings (cp. Fig. 2) the structure of the derivation is shown by explaining the influence of the rotor winding r_3 upon the stator winding s_1.

$$\psi_{s_1,r_3}(\theta, t) = L_3 \cdot i_{r_3}(t) \cos(\theta(t)) \tag{5}$$
$$\text{with } \theta = \chi(t) + \frac{k-1}{n} \cdot 2\pi = \chi(t) + \frac{2}{3} \cdot 2\pi \tag{6}$$

This analysis can be done in an analogue manner for the remaining winding systems. Expanding this approach to m stator and n rotor windings leads to the state-space model:

$$\mathbf{R}\frac{d\mathbf{x}}{dt} = \mathbf{A}\mathbf{x} + \mathbf{B}\mathbf{u} \tag{7}$$
$$\text{with } \mathbf{R} = \begin{pmatrix} \mathbf{R}_{SS} & \mathbf{R}_{SR} \\ \mathbf{R}_{RS} & \mathbf{R}_{RR} \end{pmatrix} \tag{8}$$

The input vector $\mathbf{u}$ of the state space consists of the IM terminal voltages supplied at stator u_{si} and rotor u_{ri} (for squirrel-cage IM the rotor voltages will be chosen to zero).

$$\mathbf{u} = (u_{t,s1}, \cdots u_{t,sm}, u_{t,r1}, \cdots u_{t,rn})^T \tag{9}$$

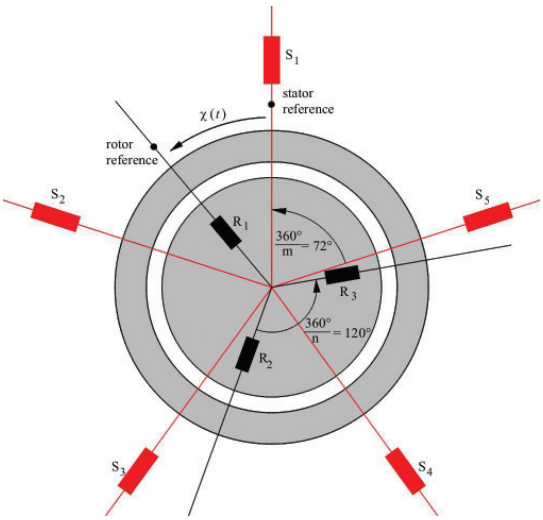

Fig. 2. Example with $m = 5$ stator and $n = 3$ rotor windings

The state vector $\mathbf{x}$ of the state space contains stator i_{si} and rotor currents i_{ri} of the IM.

$$\mathbf{x} = (i_{s1}, \cdots i_{sm}, i_{r1}, \cdots i_{rn})^T \tag{10}$$

To simplify the state-space representation differences in the inductances relevant for the induced voltages are neglected.

$$\mathbf{R}_{SS} = \mathbf{L}_{SS} + L_s \cdot \mathbf{M}_{rot,SS} \tag{11}$$

$$\mathbf{R}_{SR} = L_r \cdot N_{SR} \cdot \mathbf{M}_{rot,SR} \tag{12}$$

$$\mathbf{R}_{RS} = L_s \cdot N_{RS} \cdot \mathbf{M}_{rot,RS} = \mathbf{R}_{SR}^T$$

$$\mathbf{R}_{RR} = \mathbf{L}_{RS} + L_r \cdot \mathbf{M}_{rot,RR} \tag{13}$$

$$\mathbf{L}_{SS} = \begin{pmatrix} L_{ss1} & 0 & \cdots & 0 \\ 0 & L_{ss2} & \cdots & 0 \\ \vdots & \vdots & \ddots & \vdots \\ 0 & 0 & \cdots & L_{ssm} \end{pmatrix} \tag{14}$$

$$\mathbf{L}_{RS} = \begin{pmatrix} L_{rs1} & 0 & \cdots & 0 \\ 0 & L_{rs2} & \cdots & 0 \\ \vdots & \vdots & \ddots & \vdots \\ 0 & 0 & \cdots & L_{rsn} \end{pmatrix} \tag{15}$$

$$\mathbf{A} = \begin{pmatrix} \mathbf{A}_{SS} & \mathbf{A}_{SR} \\ \mathbf{A}_{RS} & \mathbf{A}_{RR} \end{pmatrix} \tag{16}$$

$$\mathbf{A}_{SS} = \begin{pmatrix} -R_{s1} & 0 & \cdots & 0 \\ 0 & -R_{s2} & \cdots & 0 \\ \vdots & \vdots & \ddots & \vdots \\ 0 & 0 & \cdots & -R_{sm} \end{pmatrix} \tag{17}$$

$$\mathbf{A}_{SR} = -d\frac{\mathbf{R}_{SR}}{d\chi} = \omega \cdot L_r \cdot N_{SR} \cdot \mathbf{M}_{rot,SR,sin} \tag{18}$$

$$\mathbf{A}_{RS} = -d\frac{\mathbf{R}_{RS}}{d\chi} = \omega \cdot L_s \cdot N_{RS} \cdot \mathbf{M}_{rot,RS,sin} \tag{19}$$

$$\mathbf{A}_{RR} = \begin{pmatrix} -R_{r1} & 0 & \cdots & 0 \\ 0 & -R_{r2} & \cdots & 0 \\ \vdots & \vdots & \ddots & \vdots \\ 0 & 0 & \cdots & -R_{rn} \end{pmatrix} \tag{20}$$

The terms $\mathbf{A}_{SR}$ and $\mathbf{A}_{RS}$ occur because χ is time-dependent and the derivative of this angle $\frac{d\chi}{dt} = \omega$ has to be considered (product rule).

The dimensions of the matrices depend upon the number of stator (m) and rotor (n) windings.

$$\dim(\mathbf{R}_{SS}) = \dim(\mathbf{A}_{SS}) = (m, m) \tag{21}$$

$$\dim(\mathbf{R}_{SR}) = \dim(\mathbf{A}_{SR}) = (m, n) \tag{22}$$

$$\dim(\mathbf{R}_{RS}) = \dim(\mathbf{A}_{RS}) = (n, m) \tag{23}$$

$$\dim(\mathbf{R}_{RR}) = \dim(\mathbf{A}_{RR}) = (n, n) \tag{24}$$

Finally the constraint of Kirchhoff's current law has to be considered, leading to a reduction of the $m+n$ state quantities to $m - 1 + n - 1$.

IV. Simulation Results

In this simulation a five-phase squirrel-cage induction machine (IM) is fed by a five-phase inverter. A PWM is applied transforming the sinusoidal reference voltages into five switching functions which are forwarded to the inverter phase legs. The operating point is set to $U_d = 700\,\mathrm{V}, U_{LL} = 520\,\mathrm{V}, f_s = 50\,\mathrm{Hz}, n = 3000\,\mathrm{min}^{-1}, f_{mech.} = 45\,\mathrm{Hz}, f_z = 1\,\mathrm{kHz}$ with 3300-V IGBT devices.

Figure 3 shows two of the stator currents (i_{s1}, i_{s2}) in stator-fixed reference system, two of the rotor currents (i_{r1}, i_{r2}) in rotor-fixed reference system and the negative torque $-T$ of the machine.

Before $t = 5\,\mathrm{s}$, the quantities are in steady-state, according to the specified operating point. The amplitude of the stator currents can be identified to 160 A, the rotor currents show an amplitude of 150 A.

At $t = 5\,\mathrm{s}$, the stator resistance of the first leg is set to 10000 Ohms to emulate a fault in one inverter phase leg. The simulation shows the dynamic behaviour of the induction machine currents and the torque due to this failure: It takes the system about 30 ms to reach the new steady-state. Here, the stator current i_{s1} becomes nearly zero, the rotor currents show an oscillation of about $f_r = 95\,\mathrm{Hz}$, while the torque oscillates with about $f_T = 90\,\mathrm{Hz}$ (cp. Fig.3).

V. Torque of a multi-phase machine

To evaluate the torque of a machine, first the co-energy [8] of the whole system has to be calculated. In every linear system, like the system described in this paper, the co-energy is equal to the energy. So the torque is equal to the derivative of the energy with respect to the angle χ [9].

In the case of an induction machine, the energy is a function of all currents and all inductances.

$$\begin{aligned} W' &= \frac{1}{2}L_{11}i_1^2 + \frac{1}{2}L_{22}i_2^2 + \cdots + \frac{1}{2}L_{\nu\nu}i_\nu^2 \\ &+ L_{12}i_1i_2 + L_{13}i_1i_3 + \cdots + L_{1\nu}i_1i_\nu \\ &+ L_{23}i_2i_3 + L_{24}i_2i_4 + \cdots + L_{2\nu}i_2i_\nu \\ &+ \cdots \end{aligned} \tag{26}$$

The torque can be calculated by:

$$\begin{aligned} T &= \left.\frac{\partial W'(i_\nu, L_{i,j})}{\partial(\chi)}\right|_{i_\nu = constant} \\ &= \frac{1}{2}\frac{dL_{11}}{d\chi}i_1^2 + \frac{1}{2}\frac{dL_{22}}{d\chi}i_2^2 + \cdots + \frac{1}{2}\frac{dL_{\nu\nu}}{d\chi}i_\nu^2 \\ &+ \frac{dL_{12}}{d\chi}i_1i_2 + \frac{dL_{13}}{d\chi}i_1i_3 + \cdots + \frac{dL_{1\nu}}{d\chi}i_1i_\nu \\ &+ \cdots \end{aligned} \tag{27}$$

The machine currents do not depend on the angle χ, while the inductances depend on the it. To derivative the inductances three cases have to be considered.

1) The self-inductances of the windings do not depend on the position of the rotor ($dL/d\chi = 0$), because the ASM presented in this paper has a cylindrical rotor.

$$
\begin{aligned}
\mathbf{M}_{rot,SS} &= \begin{pmatrix}
\cos\left(\frac{0}{m}\cdot 2\pi\right) & \cos\left(\frac{1}{m}\cdot 2\pi\right) & \cos\left(\frac{2}{m}\cdot 2\pi\right) & \cdots & \cos\left(\frac{m-1}{m}\cdot 2\pi\right) \\
\cos\left(\frac{m-1}{m}\cdot 2\pi\right) & \cos\left(\frac{0}{m}\cdot 2\pi\right) & \cos\left(\frac{1}{m}\cdot 2\pi\right) & \cdots & \cos\left(\frac{m-2}{m}\cdot 2\pi\right) \\
\cos\left(\frac{m-2}{m}\cdot 2\pi\right) & \cos\left(\frac{m-1}{m}\cdot 2\pi\right) & \cos\left(\frac{0}{m}\cdot 2\pi\right) & \cdots & \cos\left(\frac{m-3}{m}\cdot 2\pi\right) \\
\vdots & \vdots & \vdots & \ddots & \vdots \\
\cos\left(\frac{1}{m}\cdot 2\pi\right) & \cos\left(\frac{2}{m}\cdot 2\pi\right) & \cos\left(\frac{3}{m}\cdot 2\pi\right) & \cdots & \cos\left(\frac{0}{m}\cdot 2\pi\right)
\end{pmatrix} \\
\mathbf{M}_{rot,SR} &= \begin{pmatrix}
\cos\left(\chi+\left(-\frac{0}{m}+\frac{0}{n}\right)2\pi\right) & \cos\left(\chi+\left(-\frac{0}{m}+\frac{1}{n}\right)2\pi\right) & \cdots & \cos\left(\chi+\left(-\frac{0}{m}+\frac{n-1}{n}\right)2\pi\right) \\
\cos\left(\chi+\left(-\frac{1}{m}+\frac{0}{n}\right)2\pi\right) & \cos\left(\chi+\left(-\frac{1}{m}+\frac{1}{n}\right)2\pi\right) & \cdots & \cos\left(\chi+\left(-\frac{1}{m}+\frac{n-1}{n}\right)2\pi\right) \\
\vdots & \vdots & \ddots & \vdots \\
\cos\left(\chi+\left(-\frac{m-1}{m}+\frac{0}{n}\right)2\pi\right) & \cos\left(\chi+\left(-\frac{m-1}{m}+\frac{1}{n}\right)2\pi\right) & \cdots & \cos\left(\chi+\left(-\frac{m-1}{m}+\frac{n-1}{n}\right)2\pi\right)
\end{pmatrix} \\
\mathbf{M}_{rot,RS} &= \begin{pmatrix}
\cos\left(\chi+\left(-\frac{0}{m}+\frac{0}{n}\right)2\pi\right) & \cos\left(\chi+\left(-\frac{1}{m}+\frac{0}{n}\right)2\pi\right) & \cdots & \cos\left(\chi+\left(-\frac{m-1}{m}+\frac{0}{n}\right)2\pi\right) \\
\cos\left(\chi+\left(-\frac{0}{m}+\frac{1}{n}\right)2\pi\right) & \cos\left(\chi+\left(-\frac{1}{m}+\frac{1}{n}\right)2\pi\right) & \cdots & \cos\left(\chi+\left(-\frac{m-1}{m}+\frac{1}{n}\right)2\pi\right) \\
\vdots & \vdots & \ddots & \vdots \\
\cos\left(\chi+\left(-\frac{0}{m}+\frac{n-1}{n}\right)2\pi\right) & \cos\left(\chi+\left(-\frac{1}{m}+\frac{n-1}{n}\right)2\pi\right) & \cdots & \cos\left(\chi+\left(-\frac{m-1}{m}+\frac{n-1}{n}\right)2\pi\right)
\end{pmatrix} \\
\mathbf{M}_{rot,RR} &= \begin{pmatrix}
\cos\left(\frac{0}{n}\cdot 2\pi\right) & \cos\left(\frac{1}{n}\cdot 2\pi\right) & \cos\left(\frac{2}{n}\cdot 2\pi\right) & \cdots & \cos\left(\frac{n-1}{n}\cdot 2\pi\right) \\
\cos\left(\frac{n-1}{n}\cdot 2\pi\right) & \cos\left(\frac{0}{n}\cdot 2\pi\right) & \cos\left(\frac{1}{n}\cdot 2\pi\right) & \cdots & \cos\left(\frac{n-2}{n}\cdot 2\pi\right) \\
\cos\left(\frac{n-2}{n}\cdot 2\pi\right) & \cos\left(\frac{n-1}{n}\cdot 2\pi\right) & \cos\left(\frac{0}{n}\cdot 2\pi\right) & \cdots & \cos\left(\frac{n-3}{n}\cdot 2\pi\right) \\
\vdots & \vdots & \vdots & \ddots & \vdots \\
\cos\left(\frac{1}{n}\cdot 2\pi\right) & \cos\left(\frac{2}{n}\cdot 2\pi\right) & \cos\left(\frac{3}{n}\cdot 2\pi\right) & \cdots & \cos\left(\frac{0}{n}\cdot 2\pi\right)
\end{pmatrix} \\
\mathbf{M}_{rot,SR,sin} &= -\begin{pmatrix}
\sin\left(\chi+\left(-\frac{0}{m}+\frac{0}{n}\right)2\pi\right) & \sin\left(\chi+\left(-\frac{0}{m}+\frac{1}{n}\right)2\pi\right) & \cdots & \sin\left(\chi+\left(-\frac{0}{m}+\frac{n-1}{n}\right)2\pi\right) \\
\sin\left(\chi+\left(-\frac{1}{m}+\frac{0}{n}\right)2\pi\right) & \sin\left(\chi+\left(-\frac{1}{m}+\frac{1}{n}\right)2\pi\right) & \cdots & \sin\left(\chi+\left(-\frac{1}{m}+\frac{n-1}{n}\right)2\pi\right) \\
\vdots & \vdots & \ddots & \vdots \\
\sin\left(\chi+\left(-\frac{m-1}{m}+\frac{0}{n}\right)2\pi\right) & \sin\left(\chi+\left(-\frac{m-1}{m}+\frac{1}{n}\right)2\pi\right) & \cdots & \sin\left(\chi+\left(-\frac{m-1}{m}+\frac{n-1}{n}\right)2\pi\right)
\end{pmatrix} \\
\mathbf{M}_{rot,RS,sin} &= -\begin{pmatrix}
\sin\left(\chi+\left(-\frac{0}{m}+\frac{0}{n}\right)2\pi\right) & \sin\left(\chi+\left(-\frac{1}{m}+\frac{0}{n}\right)2\pi\right) & \cdots & \sin\left(\chi+\left(-\frac{m-1}{m}+\frac{0}{n}\right)2\pi\right) \\
\sin\left(\chi+\left(-\frac{0}{m}+\frac{1}{n}\right)2\pi\right) & \sin\left(\chi+\left(-\frac{1}{m}+\frac{1}{n}\right)2\pi\right) & \cdots & \sin\left(\chi+\left(-\frac{m-1}{m}+\frac{1}{n}\right)2\pi\right) \\
\vdots & \vdots & \ddots & \vdots \\
\sin\left(\chi+\left(-\frac{0}{m}+\frac{n-1}{n}\right)2\pi\right) & \sin\left(\chi+\left(-\frac{1}{n}+\frac{1}{n}\right)2\pi\right) & \cdots & \sin\left(\chi+\left(-\frac{m-1}{m}+\frac{n-1}{n}\right)2\pi\right)
\end{pmatrix}
\end{aligned}
\tag{25}
$$

2) The inductances which describe the effect between two windings, which do not move relative to each other, i.e. the stator or the rotor windings, are also not a function of the position of the rotor ($dL/d\chi = 0$).
3) The inductances which describe the effect between two windings, which have a relative movement to each other, i.e. a stator winding and a rotor winding (included in the matrix $\mathbf{R}_{SR}$ or $\mathbf{R}_{RS}$), depend on the position of the rotor ($dL/d\chi \neq 0$) and generate the torque of the machine.

So only the elements of the matrices $\mathbf{R}_{SR}$ or $\mathbf{R}_{RS}$ have an effect on the machine torque. The torque of an IM with m stator windings and n rotor windings can be evaluated as follows:

$$
T = \underbrace{\begin{pmatrix} i_{s1} & i_{s2} & i_{s3} & \cdots & i_{sm} \end{pmatrix}}_{1\times m} \cdot \underbrace{\frac{\partial \mathbf{R}_{SR}}{\partial \chi}}_{m\times n} \cdot \underbrace{\begin{pmatrix} i_{r1} \\ i_{r2} \\ i_{r3} \\ \vdots \\ i_{rn} \end{pmatrix}}_{n\times 1} \tag{28}
$$

VI. Conclusion

A method of modelling complex induction machines with asymmetric characteristics of all stator and rotor parameters is presented. Using this method more complex and even asymmetric machines, e.g. with 5 or 7 phases, with double-star stator windings or with asymmetric supply faults can be modelled. Based on this introduced description, the torque can be calculated using the co-energy approach [8].

Furthermore a simulation structure allowing to simulate the time behaviour of power electronic systems – e.g. for naval onboard and harbour-ship power-distribution systems – is briefly introduced.

The combination of the novel modelling method and the simulation concept presented in this paper fulfils all requirements of modern complex power-electronic topologies. The new approach enables a fast and accurate simulation featuring power-electronic power-conditioning systems controlled by independent controllers using different sampling times and switching frequencies. For this reason the chosen simulation approach is an excellent instrument supporting analysis of onboard grid stability, harbour-grid interaction and design of control algorithms for all power-conditioning devices.

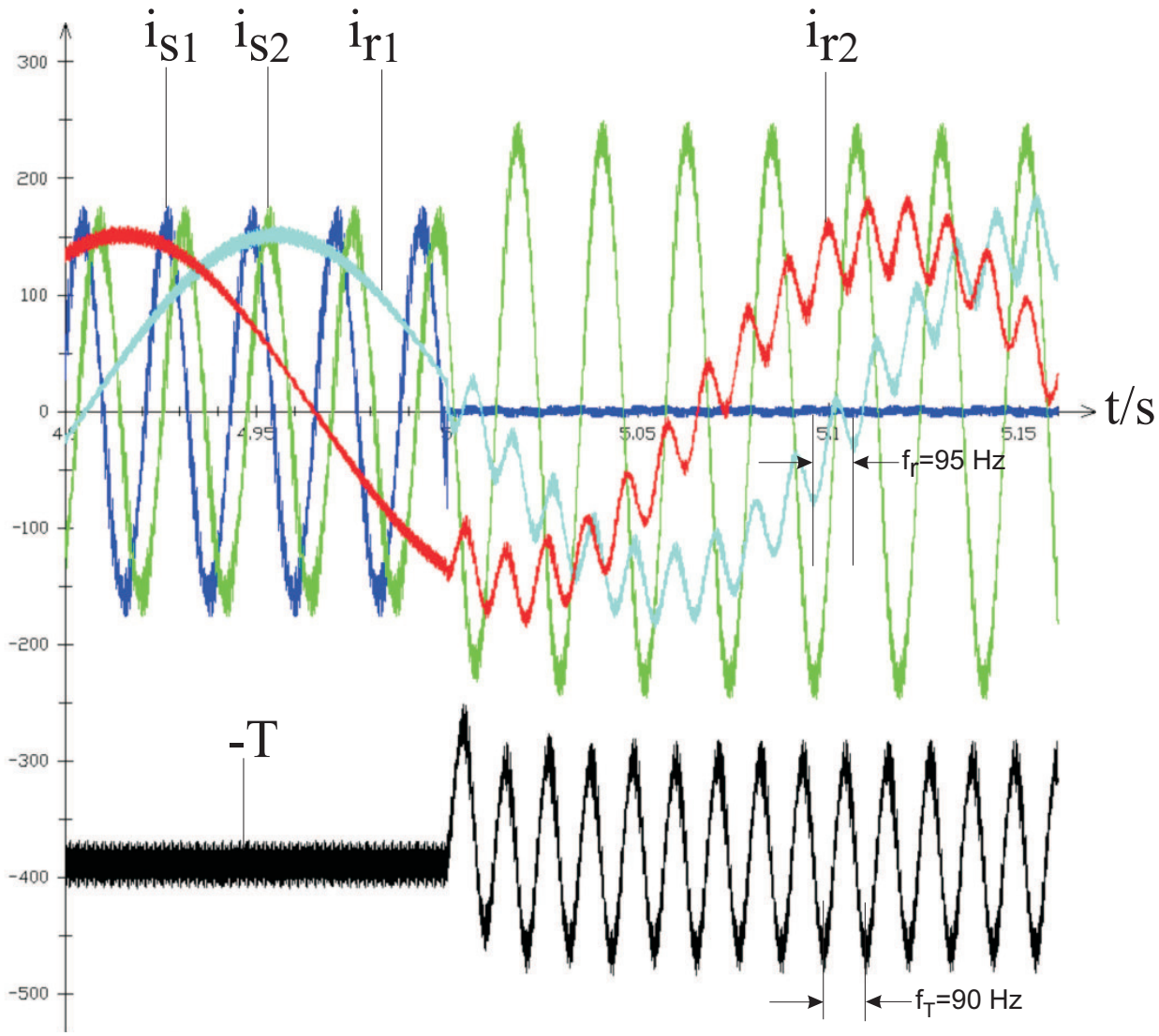

Fig. 3. Stator and rotor currents and torque of an induction machine, interruption in one inverter phase leg at $t = 5\,\mathrm{s}$.

REFERENCES

[1] C. Heising, M. Oettmeier, R. Bartelt, F. Jie, V. Staudt, and A. Steimel, "Simulation of asymmetric faults of a five-phase induction machine used in naval applications," in *35th Annual Conference of the IEEE Industrial Electronics Society (IECON)*, (Porto, Portugal), 2009.

[2] R. Bartelt, C. Heising, M. Oettmeier, V. Staudt, and A. Steimel, "Advanced simulation concept for power electronic systems applied to the 3-level npc inverter," in *35th Annual Conference of the IEEE Industrial Electronics Society (IECON)*, (Porto, Portugal), 2009.

[3] C. Heising, M. Oettmeier, R. Bartelt, V. Staudt, and A. Steimel, "Advanced simulation concept for onboard ship grids featuring complex multiterminal power-electronic systems," in *IEEE Electric Ship Technologies Symposium (ESTS)*, (Baltimore, Maryland/USA), pp. 170 – 173, 2009.

[4] C. Heising, R. Bartelt, M. Oettmeier, V. Staudt, and A. Steimel, "Simulation tool for coupled but independently controlled power-electronic systems applied to npc converters," in *Power Conversion Intelligent Motion (PCIM)*, (Nuremberg), 2010.

[5] W. Press, S. Teukolsky, W. Vetterling, and B. Flannery, *Numerical Recipes in C*. Cambridge: Cambridge University Press, 1988.

[6] V. Staudt, C. Heising, and A. Steimel, "Advanced simulation concept for power train of loco and its verification," in *ICPE 07 Conference*, (Daegu, South Korea), 2007.

[7] V. Staudt, *Zusammenhänge zwischen dem Sättigungsverhalten und den Ständerflußverkettungen von Drehfeldmaschinen*. Phd-thesis, Ruhr-University Bochum, Düsseldorf, Germany, 2002.

[8] C. Hodge, J. Flower, and A. Macalindin, "A comparison of co-energy and lorenz force based simulations of rail guns," pp. 157 –164, april 2009.

[9] A. Fitzgerald, J. Charles Kingsley, and S. D. Umans, *Electric machinery*. McGraw-Hil Higer Education, 2003.